Journal of Molecular and Cellular Cardiology 56 (2013) 91–96

Contents lists available at SciVerse ScienceDirect

Journal of Molecular and Cellular Cardiology

journal homepage: www.elsevier.com/locate/yjmcc

Original article

Microtubule proliferation in right ventricular myocytes of rats with monocrotaline-induced pulmonary hypertension

Rachel Stones [a], David Benoist [a,b], Michelle Peckham [c], Ed White [a,*]

[a] School of Biomedical Sciences & Multidisciplinary Cardiovascular Research Centre, University of Leeds, Leeds, UK
[b] Inserm U-1045, Centre de recherche Cardio-Thoracique, Université Bordeaux Segalen, &, L'Institut de Rythmologie et Modélisation Cardiaque, Université de Bordeaux, Bordeaux, France
[c] School of Molecular and Cellular Biology, University of Leeds, Leeds, UK

ARTICLE INFO

Article history:
Received 4 July 2012
Received in revised form 15 November 2012
Accepted 12 December 2012
Available online 21 December 2012

Keywords:
Pulmonary hypertension
Microtubules
Cardiac myocytes
Right ventricle
Monocrotaline

ABSTRACT

Microtubules are components of the cardiac cytoskeleton that can proliferate in response to pressure-overload in animal and human heart failure. We wished to test whether there was a proliferation of the microtubule cytoskeleton in the right ventricle of rats with pulmonary hypertension induced by monocrotaline (MCT) and whether this contributed to contractile dysfunction. Male Wistar rats were injected with 60 mg/kg of MCT in saline or an equivalent volume of saline (CON). MCT produced clinical signs of heart failure within 4 weeks of injection. Expression of right ventricular mRNA for α-tubulin was measured by real-time reverse transcription polymerase chain reaction. Free and polymerised fractions of β-tubulin protein were assessed using Western blot analysis and immunofluorescence microscopy was used to assess tyrosinated and acetylated (stabilized) microtubules. Right ventricular myocyte contraction was measured in response to the microtubule de-polymeriser colchicine (10 μmol/l for at least 1 h). Compared to CON, in MCT right ventricles there was a small but statistically significant increase in the expression of mRNA for α-tubulin ($P<0.001$); total ($P<0.05$) and polymerised fraction ($P<0.01$) of β-tubulin protein and level of acetylated tubulin ($P<0.01$). However colchicine treatment did not increase the contraction of MCT myocytes ($P>0.05$) or affect their response to increased stimulation frequency. Our observations support the hypothesis that microtubule proliferation is a common response to pulmonary hypertension in failing right ventricles but suggest that the effect this has on contraction depends upon the specific experimental or clinical conditions that prevail and the subsequent level of microtubule proliferation.

1. Introduction

Microtubules are load-bearing and load-modulated (stress-polymerised) components of the cardiac myocyte cytoskeleton [1,2]. They are protein cylinders of α and β-tubulin heterodimers, about 25 nm in diameter, aligned predominantly along the longitudinal axis of myocytes. The levels of α- and β-tubulin are closely linked. Microtubules undergo post-translational modification, such as the acetylation of Lys40, as part of a stabilization process [3]. Microtubules also interact with microtubule associated proteins (Map) that promote stability (predominantly Map4 in cardiac muscle) and with GTP-binding proteins such as G_i and G_s see [1,2,4,5]. In tissue from human sufferers of heart failure there is increased mRNA and protein levels for tubulin, e.g. [6] under conditions where wall stress is enhanced [7].

In a series of seminal studies, that included the generation of pulmonary hypertension by pulmonary artery banding, Cooper and colleagues showed that microtubule proliferation could provoke myocardial contractile dysfunction [4,5,8–10]. In their studies, depressed ejection fraction and elevated levels of cellular tubulin were seen in *in situ* whole hearts [10]. The shortening of failing myocytes was decreased by a viscous load imposed on the sarcomeres by a proliferated microtubule cytoskeleton [11] rather than by changes in Ca^{2+} handling [12]. This viscous load was relieved and shortening was restored by microtubule disruption [8,12].

However such a role for microtubules was not found in all studies [13,14] and it has been reported that pulmonary hypertension induced by alterations in the pulmonary vasculature has different outcomes to load-only elevation (pulmonary artery banding) [15]. Monocrotaline (MCT) induces pulmonary hypertension in rats. There are effects upon the pulmonary vasculature and subsequent right ventricular (RV) failure [16,17]. However the role of microtubules in this dysfunction has not been investigated. The aim of this study was to test whether microtubule proliferation occurs in the RV of MCT-treated rats and whether this is associated with the contractile dysfunction seen in this model, in order to give further insights into the response of the microtubule cytoskeleton to pressure overload and to the contractile dysfunction of the RV in pulmonary hypertension.

* Corresponding author at: School of Biomedical Sciences, Garstang Building, University of Leeds, Leeds LS29JT, UK. Tel.: +44 113 343 4248; fax: +44 113 343 4228.
E-mail address: e.white@leeds.ac.uk (E. White).

0022-2828
http://dx.doi.org/10.1016/j.yjmcc.2012.12.010

2. Methods

2.1. Animal model

All experiments were conducted in accordance with the Directive 2010/63/EU of the European Parliament and with local ethical review. Male Wistar rats (200 g) received a single intraperitoneal injection of MCT (60 mg/kg in saline) or an equivalent volume of saline (CON). Animals were weighed weekly for 3 weeks post-injection then daily. MCT-treated animals were sacrificed when they exhibited clinical signs of heart failure which included: loss of weight on successive days, dyspnea, cold extremities or lethargy. CON animals were sacrificed on equivalent days, post-injection. Blot dried heart, lung and liver weights were recorded in all animals.

2.2. Measurement of mRNA by real time reverse transcription polymerase chain reaction (RT-PCR)

RV free wall samples from 14 MCT and 12 CON rats were snap frozen in liquid nitrogen. Total RNA extraction was performed using a modified Qiagen mini-kit protocol for striated muscle and real-time RT PCR was performed using an ABI PRISM 7900HT sequence detection system (Applied Biosystems) as previously described [18,19]. The expression of gene transcripts for α-tubulin and Map4 in the test samples was normalized to an endogenous reference (18S). The normalized signal was then made relative to the normalized signal level in a corresponding calibrator sample (which is composed of cDNA from a control sample).

2.3. Western blotting

Sections of RV tissue were prepared for Western Blot analysis of tubulin as previously described [20]. Briefly, isolated hearts were flushed with a physiological solution (see below) to remove excess blood. A section of RV tissue was dissected, weighed and homogenized in an appropriate amount of microtubule stabilizing buffer (MTSB; 5 ml comprising, glycerol 50%, dimethyl sulfoxide 5%, sodium phosphate (pH 6.75) 10 mM, ethylene glycol tetraacetic acid 0.5 mM, $MgSO_4$ 0.5 mM, NP-40 detergent 1%, sodium pyrophosphate 25 mM, per 0.25 g of tissue). The MTSB was supplemented with Protease Inhibitor Cocktail (PIC, 1:200, Sigma) and phosphatase inhibitor cocktail (PPIC, 1:200, Sigma). A sample was then centrifuged at 100,000 *g* for 20 min. at 25 °C. The resulting supernatant containing the free tubulin fraction was saved. The pellet was re-suspended and homogenized on ice in the same volume of microtubule de-stabilizing buffer (MTDB; sucrose 250 mM, sodium phosphate (pH 6.75) 10 mM, $MgSO_4$ 0.5 mM, GTP 1 mM) supplemented with PIC and PPIC as before. The sample was kept on ice for 1.5 h and then centrifuged at 100,000 *g*, 4 °C for 20 min. The resulting supernatant contained the polymerised fraction of tubulin. The remaining pellet was re-suspended in MTDB and checked for any residual tubulin. Equal proportions of free and polymerised tubulin fractions were separated on 10% Tris–HCl gels under reducing conditions, this was equivalent to 20 μg of protein as determined by bicinchoninic acid assay in the free tubulin fractions. This was followed by a semi-dry transfer of the proteins onto polyvinylidene fluoride membranes and probing by antibodies (primary antibody, anti-β-tubulin antibody, 1:500, Sigma; secondary antibody; goat-anti-mouse, 1:2500, Immuno Research). Band density was determined using Scion Image for Windows (Scion Corporation, USA). Equal proportions of the free and polymerised tubulin fractions were loaded for comparison. Equivalent loading was checked by stripping and re-probing the membranes for glyceraldehyde 3-phosphate dehydrogenase (GAPDH).

2.4. Immunofluorescence microscopy

Single RV myocytes were plated onto laminin-coated coverslips, and allowed to settle for 2 h in medium. Cells were fixed in 4% paraformaldehyde for 10 min, followed by 10 min in methanol (−20 °C) or subsequent permeabilization in 0.1% Triton-X in phosphate buffered saline. Antibodies were diluted in phosphate buffered saline containing 0.1% Triton-X 100. Antibodies were mouse anti-acetylated tubulin (Sigma), rat anti-tyrosinated tubulin (Serotec) and mouse anti-β-tubulin (Sigma). Secondary antibodies were anti-mouse Alexa 546 and anti-rat Alexa 488 (Molecular probes). Cells were imaged by de-convolution microscopy using a Deltavision system (Applied Precision). In subsequent experiments, to study the effects of colchicine, a Zeiss confocal LSM700 was used. In each case exposure times were set at the start of imaging and maintained throughout. To analyse fluorescence, 3 rectangular areas were chosen at random in each cell image, and total fluorescence intensity within the rectangle was measured separately for each fluorescence channel using Image J. The background fluorescence (outside the cell) was subtracted for each image prior to analysis. For relative tubulin abundance each measurement of fluorescence was divided by the mean of the relevant CON group. To measure the effect of colchicine, fluorescence in the presence of colchicine was divided by the mean of the relevant vehicle group. Data were analysed using Graph Pad Prism.

2.5. Myocyte shortening

Single RV myocytes were isolated using a collagenase digestion technique as previously described [21]. The experimental solution contained (mmol/l) NaCl 137, KCl 5.4, NaH_2PO_4 0.33, $MgCl_2$ 0.5, HEPES 5, glucose 5.6, $CaCl_2$ 1, and pH 7.4. Cells were exposed to the microtubule disruptor colchicine (10 μM) dissolved in methanol (0.1% vol/vol in experimental solution) or to vehicle in solution for at least 1 h [8,22] before transferring to the experimental chamber of an inverted microscope (Nikon Diaphot). Cells were superfused with experimental solution containing vehicle in the presence or absence of colchicine. Cells were stimulated by external platinum electrodes to contract to steady state at stimulation frequencies of 1 Hz and 5 Hz. Cell shortening and resting sarcomere length were measured with a video edge detection device (Ionopix, Milton, MA). The index of contraction was shortening as a % of resting cell length. The maximum rate of sarcomere shortening was measured from the d/dt derivative of the cell length trace. All treatments and experiments were carried out at 37 °C.

2.6. Statistics

All data are expressed as mean ± sem. Two-way analysis of variance (ANOVA), two-way repeated measures ANOVA, unpaired Student's t-tests or non-parametric equivalents were performed as appropriate. Statistically significant difference was assumed if $P<0.05$.

3. Results

3.1. Microtubule proliferation in RV myocytes from MCT-treated rats

MCT treated animals had significantly greater heart, lung and liver weight to body weight ratios (Fig. 1A) and RV weight to LV weight (Fig. 1B). Consistent with a proliferation of the microtubule cytoskeleton in MCT hearts, real time RT-PCR analysis revealed a significantly elevated expression of mRNA for α-tubulin ($P<0.001$, Fig. 2). However mRNA for Map4 was not increased (Fig. 2). Western blot analysis showed significantly elevated levels of total tubulin protein ($P<0.05$) and polymerised tubulin fraction ($P<0.01$) in the RV of MCT hearts (Fig. 3). Immunofluorescence microscopy on single

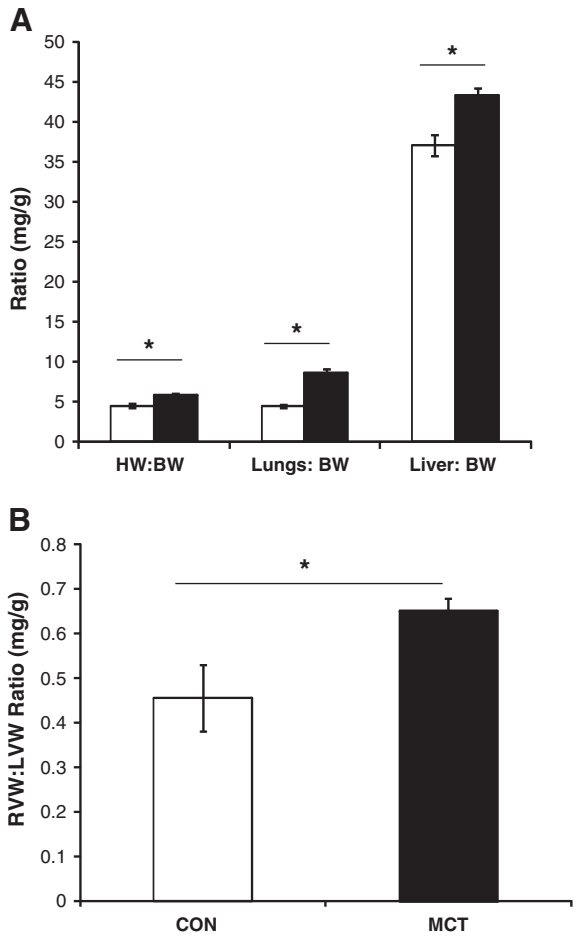

Fig. 1. Right ventricular hypertrophy in MCT-treated animals. (A) Heart weight (HW), lungs and liver weight to body weight (BW) ratios and (B) right ventricular weight (RVW) to left ventricular weight (LVW) ratio, for CON (□) and MCT treated (■) rats. MCT treated rats had increased HW:BW, Lungs:BW, Liver:BW and RVW:BW (*P<0.001 unpaired *t*-test, n = 6 each group).

myocytes (Figs. 4A & C) found that the level of tyrosinated tubulin was not statistically increased in MCT myocytes but β-tubulin (P<0.01) and acetylated (stabilized) tubulin (P<0.001) were increased (Fig. 4 C). There was a significant decrease in the level of β-tubulin (P<0.001) and tyrosinated tubulin (P<0.01 CON, P<0.001 MCT)

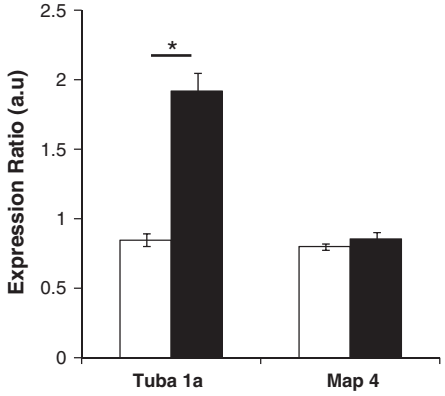

Fig. 2. mRNA expression of microtubule related proteins in MCT right ventricles. There was an increase in the expression of mRNA encoding for α-tubulin in the right ventricle of MCT treated (■) rats compared to CON (□) but expression of mRNA for microtubule associated protein (Map4) was not significantly increased (*P<0.001, unpaired *t*-test, n = 14 MCT, n = 12 CON, results were normalized to expression of 18S).

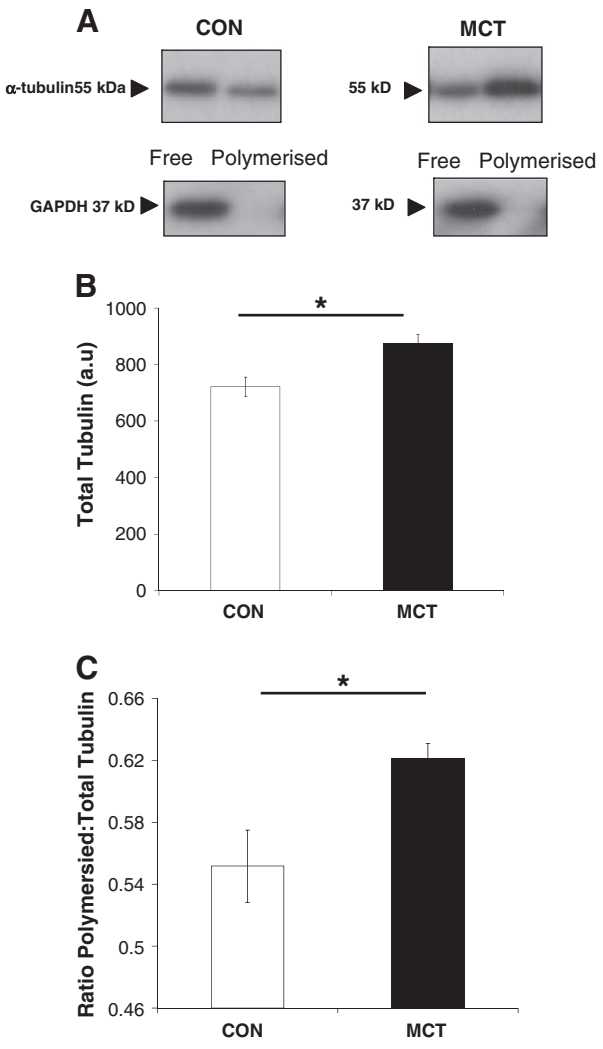

Fig. 3. Increased tubulin protein in MCT right ventricles. (A) Western blot showing increased levels of β-tubulin in the right ventricle of MCT-treated rats. (B) Total tubulin and (C) ratio of polymerised to total tubulin for CON (□) and MCT treated (■) rats mean ± sem. Equivalent loading was checked by re-probing for GAPDH. There was a statistically significant increase in total tubulin and the fraction of polymerised β-tubulin in the MCT treated RV tissue compared to CON (B *P<0.05, C *P<0.01, unpaired *t*-test, n = 6 each group).

following treatment with colchicine. The effect of colchicine on β-tubulin was significantly greater in CON than MCT myocytes (P<0.001). There was no effect of colchicine on acetylated tubulin (Fig. 4D).

3.2. Lack of effect of microtubule disruption on shortening of RV myocytes from MCT-treated rats

In unstimulated cells we observed a significantly shorter resting sarcomere length in MCT myocytes (P<0.001). Exposure to colchicine did not affect the resting sarcomere length of either CON (vehicle 1.91 ± 0.01 μm; colchicine 1.93 ± 0.01 μm, n = 24 cells each, P > 0.05) or MCT myocytes (vehicle 1.79 ± 0.01 μm; colchicine 1.78 ± 0.01 μm, n = 26–28 cell, P > 0.05).

When stimulated, shortening was significantly greater in MCT myocytes at a stimulation frequency of 1 Hz (Figs. 5A & B) but not at 5 Hz (Figs. 5A & D). Increased stimulation frequency caused an increase in the shortening of CON myocytes but a decrease in the shortening of MCT myocytes, this difference in response was statistically significant (Fig. 5F). Exposure to colchicine did not alter any of these parameters.

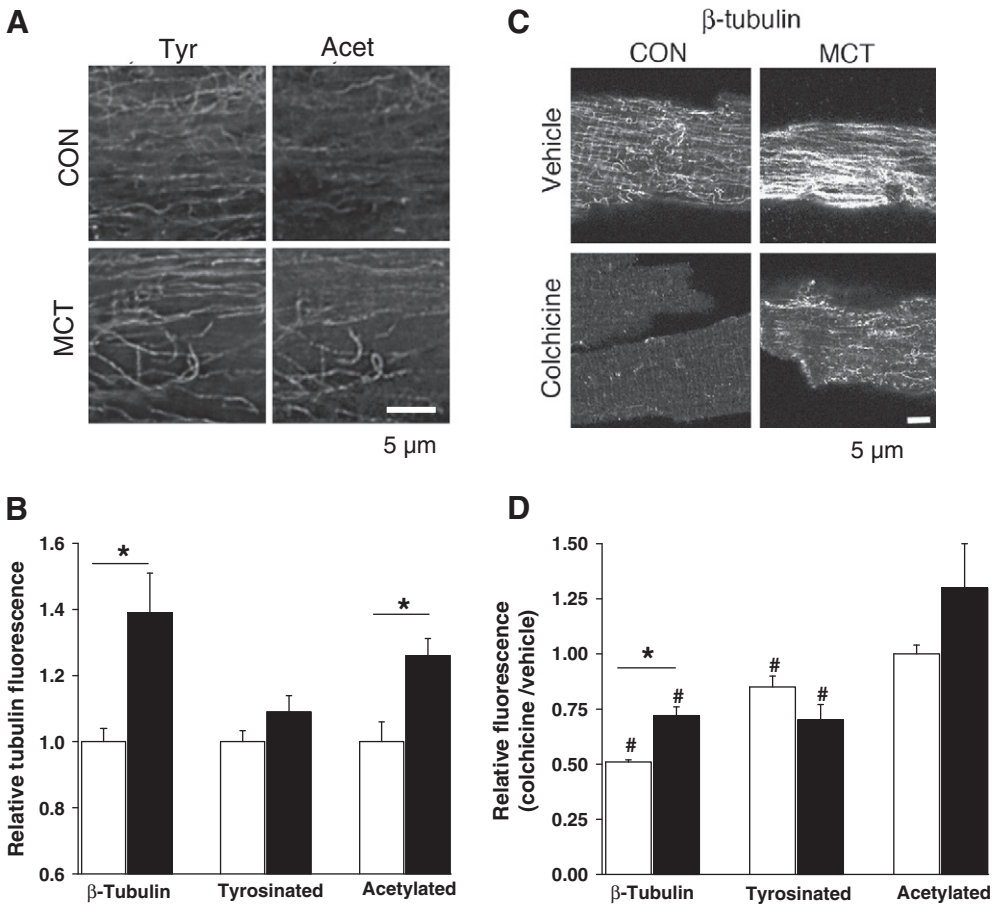

Fig. 4. Immunofluorescence imaging of tubulin in cardiac myocytes and the response to colchicine treatment. (A) Tubulin cytoskeleton in RV myocytes from control (CON) and MCT-treated hearts. Images show labelling for tyrosinated tubulin (Tyr) and acetylated tubulin (Acet). (B) Relative tubulin abundance (see Methods). Compared to CON (□), in MCT (■) myocytes, there was a statistically significant increase in β-tubulin (*P<0.001, n = 48 CON and 36 MCT) and acetylated tubulin (*P<0.001, n = 54 CON and 48 MCT) but no difference in tyrosinated tubulin (P > 0.05 n = 54 CON and 48 MCT). (C) Images for β-tubulin in the presence or absence of colchicine. (D) Effect of exposure to colchicine (see Methods). There was a statistically significant decrease in β-tubulin in both CON (□) and MCT (■) myocytes treated with colchicine (# P<0.001, n = 33 CON and 27 MCT). The effect on CON myocytes was significantly greater than on MCT myocytes(*P<0.001). There was a significant decrease in tyrosinated tubulin in both CON (# P<0.01, n = 27) and MCT (# P<0.001, n = 21). Colchicine did not decrease acetylated tubulin (P > 0.05, n = 27 CON and 21 MCT).

The rate of sarcomere shortening was not different between CON or MCT myocytes at 1 Hz (Fig. 5C) but was greater in CON myocytes at 5 Hz (Fig. 5E). There was an increase in the rate of sarcomere shortening in CON myocytes when stimulation frequency was increased but a decrease in rate in MCT myocytes. This difference in response was statistically significant (Fig. 5G).

4. Discussion

4.1. Evidence for increased wall stress and proliferated microtubules in MCT-treated hearts

The principle novel findings of our study are that the microtubule cytoskeleton of RV myocytes from MCT-treated animals is proliferated, with some evidence of increased stabilization (acetylated tubulin), but this proliferation does not contribute to the contractile dysfunction seen in these myocytes.

It is thought that pressure-induced microtubule proliferation is triggered when cardiac hypertrophy cannot prevent an increase in ventricular wall stress [4,5]. Wall stress (σ) can be calculated as σ = pr/2h where p = trans-wall pressure difference; r = radius of curvature and h = wall thickness. We have measured peak systolic pressure in CON hearts to be 24 mmHg and 79 mmHg in MCT hearts [19]; RV wall thicknesses as 0.63 mm (CON) and 1.4 mm (MCT) and a mid-line RV radius of curvature of 6.5 mm (CON) and 7.0 mm (MCT) [23]. On the simplified assumptions that the RV cross-section is circular and the RV wall is solid, substitution of these values into the above equation gives a 59% increase in wall stress in the RV of MCT compared to CON hearts. Thus there appears to be a feasible trigger for microtubule proliferation in the MCT model. Consistent with this prediction, we found evidence for increased tubulin mRNA; total and polymerised tubulin protein and post-translational stabilization by acetylation.

4.2. Reasons for lack of effect of proliferated microtubules on contraction of MCT myocytes

However, microtubule disruption did not increase shortening amplitude in MCT myocytes nor did it increase the rate of sarcomere shortening. This may stem from the fact that the contractile phenotypes of pulmonary artery banding studies and MCT-treated rats are different. Banding consistently leads to a reduction in myocyte contraction at relatively low stimulation frequencies [5,8]. In contrast we find that at 1 Hz cell shortening in MCT treated myocytes is enhanced but falls steeply with increased stimulation frequency [23] (and this study Fig. 5). As stimulation frequency increases, resting $[Ca^{2+}]i$ levels increase and the diastolic cell length shortens. It was conceivable that a mechanism restricting sarcomere shortening (microtubule proliferation) could become more pronounced at shorter diastolic sarcomere lengths as the compressive forces on

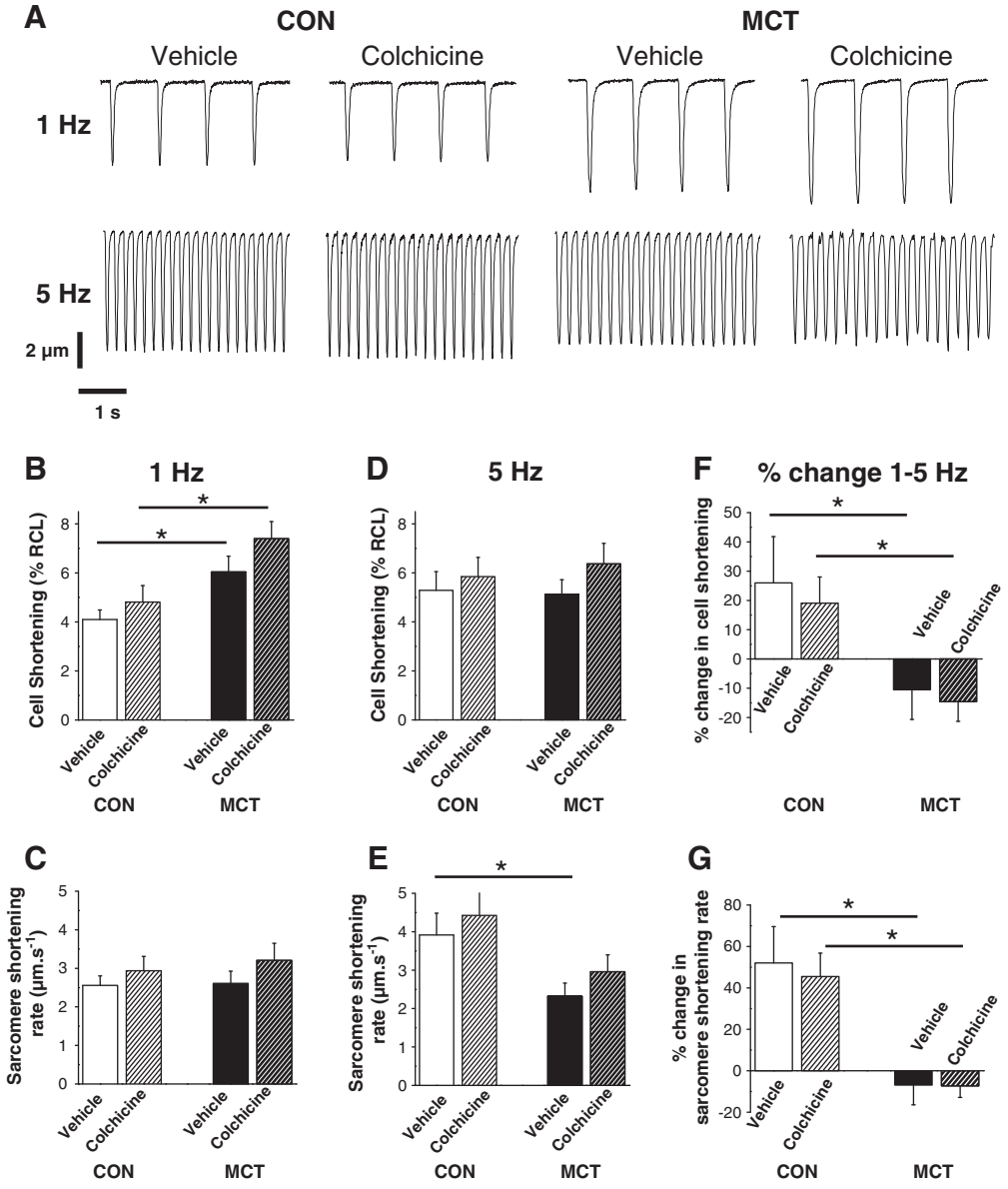

Fig. 5. Contraction in single right ventricular cardiac myocytes. (A) Representative traces of cell shortening from control (CON) and MCT-treated myocytes exposed to colchicine or vehicle at stimulation frequencies of 1 Hz and 5 Hz. Mean ± sem for % cell shortening or rate of sarcomere shortening at 1 Hz (B and C) and 5 Hz (D and E). Change in % cell shortening and rate of sarcomere shortening when stimulation frequency was increased (F and G). Cell shortening was significantly greater in MCT cells at 1 Hz (*P<0.05) but not at 5 Hz. Increasing stimulation frequency increased the amplitude and rate of shortening in CON cells but reduced these in MCT-treated cells. Colchicine did not affect these responses (*P<0.05 in B, E and F; P<0.01 in B, colchicine and in G, 2-way ANOVA, n = CON 19 and 15 MCT cells).

microtubules increase. Thus there was the possibility that microtubules play a role in the steep stimulation frequency dependent fall in contraction seen in MCT myocytes (and many other heart failure models). However our experimental evidence suggests this is not the case.

One factor that may explain the lack of effect of microtubule disruption upon contraction is that although we saw statistically significant increases in tubulin mRNA and protein the increase was less than that previously reported for pulmonary artery banding. Comparing β-tubulin measured by Western blotting, we saw a 21% increase in total tubulin and a 7% increase in the polymerised fraction while Tsutsui et al. [8] reported 100% increase in total tubulin with a maintained polymerised fraction, in response to 4 weeks pulmonary artery banding in cats. In addition we saw no increase in mRNA expression of Map4. Decoration of microtubules with Map4 is thought to be an important factor in their stabilization and effects upon contraction [20]. Therefore we conclude that although there is some proliferation and stabilization of the microtubule cytoskeleton in response to MCT this is not large enough to modulate contraction.

However, in making this conclusion we note that the study of Ishibashi et al. [24] reported an increase in total tubulin of 30% and an increase in the polymerised fraction of 28% following 4 weeks of abdominal aortic constriction in rats. These responses are closer to those we observed but in that study [24] 30 min exposure to 1 µM colchicine had a beneficial effect upon myocyte contraction.

The increase in wall stress in response to MCT may not be as great as seen in previous banding studies and wall stress is thought to be a key factor in the microtubule response [5]. It may also be relevant that volume overload is reported to have no effects upon the microtubule cytoskeleton [8] and the MCT model causes both volume and pressure overload.

While changes in $[Ca^{2+}]i$ handling are not thought to be important in the contractile response of some artery banding models [8,12], they are found in the MCT model. We have previously reported that there

is a steep action potential duration restitution and Ca^{2+} transient amplitude restitution, in the presence of reduced sarcoplasmic reticulum Ca^{2+} pump function [23]. It now seems likely that these changes in Ca^{2+}-handling rather than a densification of the microtubule cytoskeleton are principally responsible for the steep fall in shortening with increased stimulation frequency. Decreased resting sarcomere length was observed in MCT myocytes, this is thought to be due to a Ca^{2+}-independent mechanism [25] and our observations now show that this mechanism is not related to microtubule proliferation.

4.3. Specific microtubule populations

The effect of colchicine on total (β-) tubulin was greatest in CON myocytes. This may be explained by the increased levels of stabilised microtubules in MCT myocytes. We observed these microtubules to be resistant to a short destabilising treatment, consistent with previous findings [3]. The response of tyrosinated-tubulin to both MCT and colchicine treatment was small compared to β-tubulin. This is somewhat surprising and may suggest that non-specific fluorescence was dampening the responsiveness of the tyrosinated-tubulin antibody. We did see increased acetylation of MCT microtubules and when considering the role of microtubules in myocytes it is worth noting that they play a major role in cell trafficking and it has been shown there is increased selection of acetylated microtubules by molecular motors [26].

4.4. Conclusions

Our findings in MCT-induced pulmonary hypertensive rats support the theory, developed in pulmonary arterial banding models, that increased ventricular wall stress will provoke the proliferation of microtubules in failing RV myocytes. However, while microtubule proliferation has been shown to have a major impact on contraction in some models, this is not the case in the MCT model, we suggest this is because the increase in microtubules is not great enough to affect contraction. This leads to the conclusion that the major impact upon contraction in this model is via regulation of $[Ca^{2+}]i$ handling rather than microtubule proliferation. Our findings indicate that the impact of microtubule proliferation upon contraction is likely to depend upon the prevailing experimental or clinical conditions and the subsequent level of microtubule proliferation.

Disclosure statement

None.

Acknowledgements

Supported by the British Heart Foundation grant PG/08/027/24774 to EW. D.B. was an Emma and Leslie Reid Ph.D. student.

References

[1] Calaghan SC, Le Guennec JY, White E. Cytoskeletal modulation of electrical and mechanical activity in cardiac myocytes. Prog Biophys Mol Biol 2004;84:29–59.
[2] White E. Mechanical modulation of cardiac microtubules. Pflugers Arch 2011;462:177–84.
[3] Belmadani S, Pous C, Fischmeister R, Mery PF. Post-translational modifications of tubulin and microtubule stability in adult rat ventricular myocytes and immortalized HL-1 cardiomyocytes. Mol Cell Biochem 2004;258:35–48.
[4] Cooper G. Cardiocyte cytoskeleton in hypertrophied myocardium. Heart Fail Rev 2000;5:187–201.
[5] Cooper G. Cytoskeletal networks and the regulation of cardiac contractility: microtubules, hypertrophy, and cardiac dysfunction. Am J Physiol Heart Circ Physiol 2006;291:H1003–14.
[6] Heling A, Zimmermann R, Kostin S, Maeno Y, Hein S, Devaux B, et al. Increased expression of cytoskeletal, linkage, and extracellular proteins in failing human myocardium. Circ Res 2000;86:846–53.
[7] Zile MR, Green GR, Schuyler GT, Aurigemma GP, Miller DC, Cooper G. Cardiocyte cytoskeleton in patients with left ventricular pressure overload hypertrophy. J Am Coll Cardiol 2001;37:1080–4.
[8] Tsutsui H, Tagawa H, Kent RL, McCollam PL, Ishihara K, Nagatsu M, et al. Role of microtubules in contractile dysfunction of hypertrophied cardiocytes. Circulation 1994;90:533–55.
[9] Tagawa H, Koide M, Sato H, Zile MR, Carabello BA, Cooper G. Cytoskeletal role in the transition from compensated to decompensated hypertrophy during adult canine left ventricular pressure overloading. Circ Res 1998;82:751–61.
[10] Koide M, Hamawaki M, Narishige T, Sato H, Nemoto S, DeFreyte G, et al. Microtubule depolymerization normalizes in vivo myocardial contractile function in dogs with pressure-overload left ventricular hypertrophy. Circulation 2000;102:1045–52.
[11] Yamamoto S, Tsutsui H, Takahashi M, Ishibashi Y, Tagawa H, Imanaka-Yoshida K, et al. Role of microtubules in the viscoelastic properties of isolated cardiac muscle. J Mol Cell Cardiol 1998;30:1841–53.
[12] Zile MR, Koide M, Sato H, Ishiguro Y, Conrad CH, Buckley JM, et al. Role of microtubules in the contractile dysfunction of hypertrophied myocardium. J Am Coll Cardiol 1999;33:250–60.
[13] Collins JF, Pawloski-Dahm C, Davis MG, Ball N, Dorn GW, Walsh RA. The role of the cytoskeleton in left ventricular pressure overload hypertrophy and failure. J Mol Cell Cardiol 1996;28:1435–43.
[14] Bailey BA, Dipla K, Li S, Houser SR. Cellular basis of contractile derangements of hypertrophied feline ventricular myocytes. J Mol Cell Cardiol 1997;29:1823–35.
[15] Bogaard HJ, Natarajan R, Henderson SC, Long CS, Kraskauskas D, Smithson L, et al. Chronic pulmonary artery pressure elevation is insufficient to explain right heart failure. Circulation 2009;120:1951–60.
[16] Hessel MH, Steendijk P, den Adel B, Schutte CI, van der Laarse A. Characterization of right ventricular function after monocrotaline-induced pulmonary hypertension in the intact rat. Am J Physiol Heart Circ Physiol 2006;291:H2424–30.
[17] Hardziyenka M, Campian ME, de Bruin-Bon HA, Michel MC, Tan HL. Sequence of echocardiographic changes during development of right ventricular failure in rat. J Am Soc Echocardiogr 2006;19:1272–9.
[18] Stones R, Billeter R, Zhang H, Harrison S, White E. The role of transient outward K+ current in electrical remodelling induced by voluntary exercise in female rat hearts. Basic Res Cardiol 2009;104:643–52.
[19] Benoist D, Stones R, Drinkhill M, Bernus O, White E. Arrhythmogenic substrate in hearts of rats with monocrotaline-induced pulmonary hypertension and right ventricular hypertrophy. Am J Physiol Heart Circ Physiol 2011;300:H2230–7.
[20] Sato H, Nagai T, Kuppuswamy D, Narishige T, Koide M, Menick DR, et al. Microtubule stabilization in pressure overload cardiac hypertrophy. J Cell Biol 1997;139:963–73.
[21] McCrossan ZA, Billeter R, White E. Transmural changes in size, contractile and electrical properties of SHR left ventricular myocytes during compensated hypertrophy. Cardiovasc Res 2004;63:283–92.
[22] Calaghan SC, Le Guennec JY, White E. Modulation of Ca(2+) signaling by microtubule disruption in rat ventricular myocytes and its dependence on the ruptured patch-clamp configuration. Circ Res 2001;88:E32–7.
[23] Benoist D, Stones R, Drinkhill MJ, Benson AP, Yang Z, Cassan C, et al. Cardiac arrhythmia mechanisms in rats with heart failure induced by pulmonary hypertension. Am J Physiol Heart Circ Physiol 2012;302:H2381–95.
[24] Ishibashi Y, Tsutsui H, Yamamoto S, Takahashi M, Imanaka-Yoshida K, Yoshida T, et al. Role of microtubules in myocyte contractile dysfunction during cardiac hypertrophy in the rat. Am J Physiol 1996;271:H1978–87.
[25] Benoist D, Stones R, White E. Ca^{2+}-independent decrease in resting sarcomere length in rat failing right ventricular myocytes. Biophys J 2012;201:352a–3a [abstract].
[26] Dunn S, Morrison EE, Liverpool TB, Molina-Paris C, Cross RA, Alonso MC, et al. Differential trafficking of Kif5c on tyrosinated and detyrosinated microtubules in live cells. J Cell Sci 2008;121:1085–95.